The International Journal of Advanced Manufacturing Technology (2018) 97:1627–1635
https://doi.org/10.1007/s00170-018-2044-4

ORIGINAL ARTICLE

An active manufacturing method of surface micro structure based on ordered grinding wheel and ultrasonic-assisted grinding

ChangShun Chen[1] · JinYuan Tang[1] · HaiFeng Chen[2] · Bo Zhao[3]

Received: 10 August 2017 / Accepted: 16 April 2018 / Published online: 30 April 2018

Abstract
At present, many studies have shown that crosshatch micro structures can effectively improve surface performance. This paper presents a method for manufacturing micro structure based on ultrasonic-assisted grinding (UAG) and ordered grinding wheel. Firstly, the parameters of ordered grinding wheel and the surface characteristic parameters in relation to working performance are proposed. According to the kinematics of grinding, the governing equation between the surface characteristic parameters and the machining parameters is established. Based on the proposed characteristic parameters, the pattern parameters and machining parameters are inversely solved by the governing equation. The crosshatch micro structure manufacturing based on ordered grinding wheel and ultrasonic-assisted grinding is achieved, and because the fabrication technology of the grinding wheel is not mature, its correctness and feasibility are preliminary verified by the numerical simulation method and grinding experiment. The paper method is original for the active manufacturing of the crosshatch micro structure and is of reference value for the micro structure active manufacturing.

Keywords Ordered grinding wheel · Ultrasonic-assisted grinding · Crosshatch micro structure · Active manufacturing

1 Introduction

Along with the progress of science and technology, the grinding process has changed from precision forming manufacturing to surface property manufacturing, and active manufacturing of the surface micro structure is one of the realization ways. Active manufacturing means establishing a quantitative relationship between the characteristic parameters of the surface micro structure and the service performance based on the workpiece service performance requirements. Besides, to achieve the active manufacturing of the micro structure based on the service performance, it is also required to put forward some micro structure characteristic parameters according to the design-manufacturing evaluation value, and construct the design method about micro-surface with the predictable service performance. Research shows that a good surface micro structure can effectively improve the lubrication, friction, and other service performance indicators. Therefore, the research about the active manufacturing of the workpiece surface micro structure is of great significance [1–3]. The researches about properties of rough surface and characterization of the surface microstructure we have done are the basis of this paper [4–6].

As an orderly micro structure, the crosshatch micro structure has been widely used in the industrial field due to its excellent performance. Min-soo Suh [7, 8] studied the effect of the width and angle of the crosshatch pattern on the surface friction performance and took these parameters as the design evaluation parameters in the crosshatch pattern. Sihuan Yuan [9] studied the effect of sliding direction on the surface friction coefficient and simulated the process with the finite element software to verify its correctness. In addition, in actual engineering applications, the honing crosshatch is conducive to the storage and preservation of lubricating oil and can withstand great load with good wear resistance [10].

There are many ways for the processing of crosshatch micro structure. Klink and Sandhof proposed the laser honing technology to manufacture the crosshatch micro structure and applied for a patent in the USA and the European community

✉ HaiFeng Chen
ccscsu@163.com

[1] State Key Laboratory of High Performance Complex Manufacturing, Central South University, Changsha 410083, Hunan, China

[2] Hunan Provincial Key Laboratory of High Efficiency and Precision Machining of Difficult-to-Cut Materials, Hunan University of Science and Technology, Xiangtan 411201, Hunan, China

[3] Henan Polytechnic University, Jiaozuo 454000, Henan, China

[11]. Min-soo Suh [7, 8] used the laser mask manufacturing to fabricate the crosshatch micro structure which has excellent machining precision. In addition, EDM technology is also used in the manufacturing of such micro structures, but the processing dimensions are larger [12]. The abovementioned surface machining technologies are all added to the existing process to complete the processing of the micro structure, thus greatly increasing the processing cost and time.

Yan Wang [13] found that the crosshatch micro structure of the ultrasonic grinding surface would appear in some working conditions when he conducted some ultrasonic grinding researches about the titanium, and that the crosshatch micro structure has different characteristics for different parameters. Tawakoli T [14] studied surface roughness of the crosshatch pattern in ultrasonic-assisted grinding (UAG) considering the overlapped grinding trajectories. HaiFeng Chen [4] built the numerical model of the UAG workpiece surface and did some experimental researches to verify its correctness. However, crosshatch pattern just appear sometimes because of the randomly distributed abrasive grains in most of the grinding wheel, which is not suitable for the active manufacturing of the crosshatch micro structure. And the improvement of the preparation technology of the grinding wheel with a defined grain pattern provides convenience for the controllable manufacturing of the grinding surface.

The above literature analysis shows that the main problems existing in the study of the active manufacturing of the micro crosshatch structure is that the current manufacturing methods are based on the existing processing technology added an additional process, increasing the processing time and cost.

In this paper, the surface micro structure characteristic parameters in the UAG are proposed. Based on the grinding wheel with a defined grain pattern, the governing equation of the characteristic parameters is studied. Finally, the controllable and active manufacturing of the flat surface micro structure based on the ordered grinding wheel and UAG is achieved.

2 Ordered grinding wheel and UAG workpiece surface parametric representation

2.1 Modeling of single abrasive grain

For the modeling of a single abrasive grain, many researchers [15–18] assume the abrasive grain is spherical, conical, truncated cone, polyhedron, or in other shapes. The single abrasive grain is obtained by using a Veeco Wyko NT9100 to observe the single CBN abrasive sample (the grit size is 100/120) as shown in Fig. 1. Figure 1 shows that the most obvious feature of a single abrasive grain is its prominent edge for which Malkin [19] found that the average tool rake angle of abrasive grains in the grinding process is − 60°. Therefore, we assume that the abrasive grain is a cone with an apex angle of 60°.

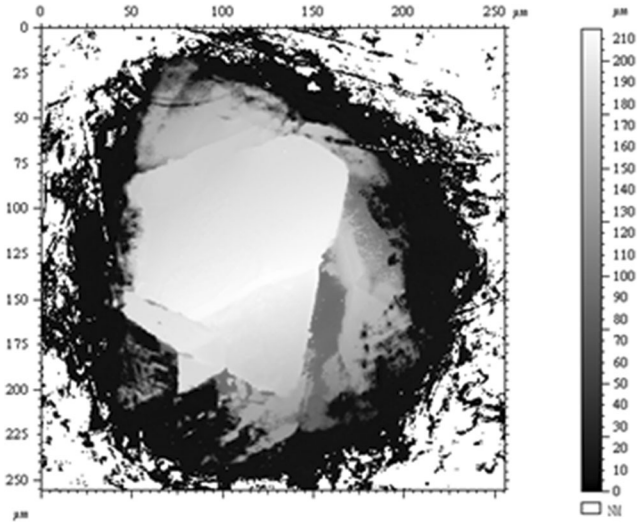

Fig. 1 Single CBN abrasive grain

2.2 Modeling of grinding wheel based on four parameters

At present, for most grinding wheels, the abrasive grains are randomly distributed on the surface of the grinding wheel, and active grains account for a small part of all grains. A large number of useless abrasive grains not only increase the cost of grinding wheels but also shrink the space for holding chips, which increases the grinding force and reduces the service life of grinding wheels. According to the Bears de company [20], the service life of the grinding wheel with a defined grain pattern is several times longer than that of the conventional grinding wheel at the same processing level.

According to the current ordered wheel production process, the grain configurations on the grinding wheel surface are phyllotactic configuration as shown in Fig. 2. The line distance D_x, grain distance within lines D_z, line angle a, and axial grain displacement between lines D_{zv} are 800 μm, 300 μm, 42.5°, 300 μm respectively.

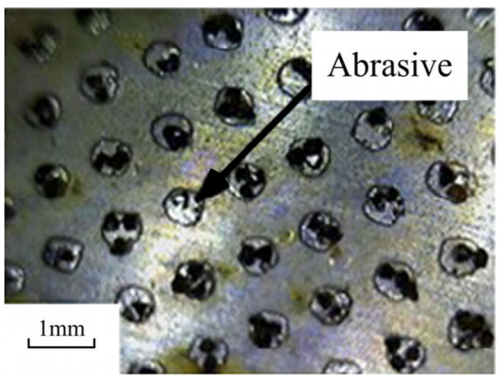

Fig. 2 Actual surface morphology of ordered grinding wheel

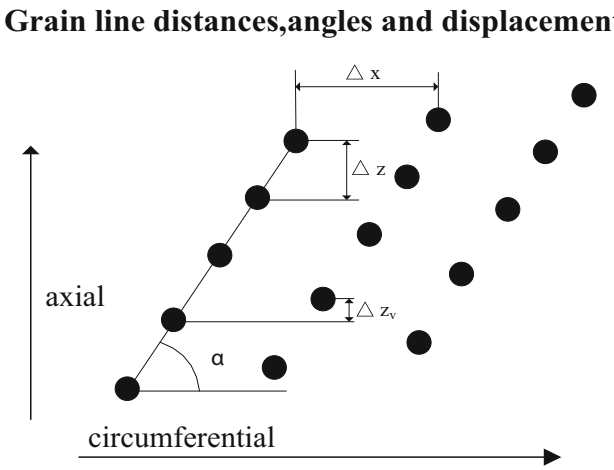

Fig. 3 Notation of modeled grain patterns [21, 22]

The design and the notation of the grain pattern are depicted in Fig. 3 [21] with four pattern parameters: line distance Δx, grain distance within lines Δz, line angle a, and axial grain displacement between lines Δz_v. According to the experimental study conducted by JC Aurich [22], the line angle is set to 50° in this paper.

As research shows that the surface roughness of the workpiece decreases with the decrease of the grain distance within lines Δz [23], the pattern is set to a dense arrangement. Finally, the grit size is set to 100 and the axial distance is 400 μm. Another two parameter settings will be mentioned in the next section.

2.3 Modeling of crosshatch micro structure

According to the characterization of the microstructure of the reticulum in [7–9], we propose the three parameters which are most closely related to the performance of the crosshatch micro structure as the reticular microstructure design index, including angle of crosshatch pattern, peak interval, angle between processing texture direction, and sliding direction. The specific diagram is shown in the following (Fig. 4).

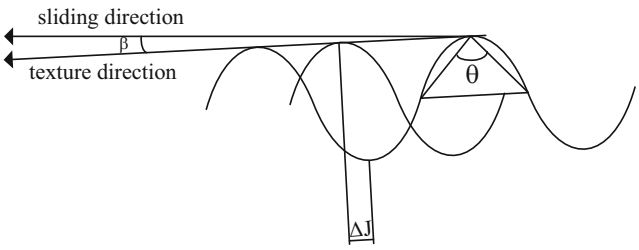

Fig. 4 Schematic of crosshatch micro structure characterization parameters

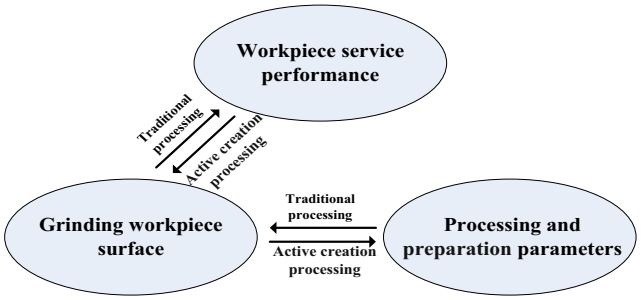

Fig. 5 Comparison of traditional processing and active manufacturing processing

3 Governing equation of active manufacturing of crosshatch micro structure

Figure 5 shows the difference between the traditional processing method and the active manufacturing method. In the traditional processing method, the grinding parameters and grinding wheel preparation parameters are set first and then the service performance of the processed workpiece is studied, but the relationship between the machining parameters and the service performance of the workpiece is not revealed. On contrary, in active manufacturing processing, the workpiece surface characteristic parameters related to the service performance are set first and then the grinding parameters and grinding wheel preparation parameters are reversely deduced by combining with grinding kinematics so that controllable and active

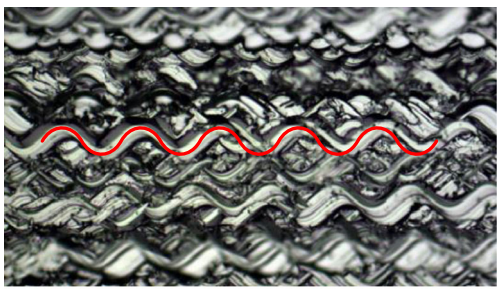

(a) Sine shape crosshatch grinding trajectory

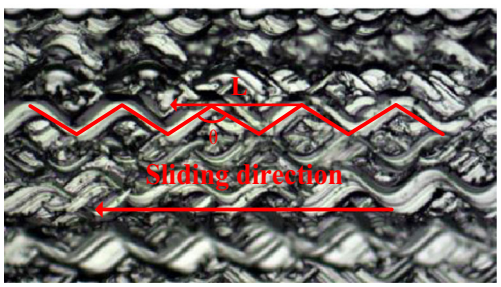

(b) Linear crosshatch grinding trajectory

Fig. 6 Simplified diagram of axis UAG surface

manufacturing of the service performance is achieved. This can meet the increasing demands of the workpiece for the service performance. The following is mainly to study the mapping relationship between the process parameters, pattern parameters, and micro structure characteristic parameters.

In order to link the axial UAG surface and the linear crosshatch micro structure together, the structure of the grinding surface will be simplified into a linear crosshatch micro structure (Fig. 6).

3.1 Governing equation of angle of crosshatch pattern

Min-soo Suh [8] found that the friction coefficient and wear rate of the surface friction pair are small when the angle of crosshatch pattern is 150°. Therefore, the angle of crosshatch pattern is set to 150°.

As shown in Fig. 7, the trajectory of abrasive grains in the axial UAG is established with two coordinate systems. The origin of frame {O} is fixed in space at the center and front of the grinding wheel. The origin of frame {G} is located at the front left end of the workpiece and is being translated with respect to frame {O} by the motion of the work table. These frames are initially separated by distances y_0 and (R-d) along Y and Z axes respectively, where y_0 is an arbitrary starting distance, R is the nominal radius of the grinding wheel, and d is the depth of cut.

According to the initial position of the abrasive grain, the cutting speed of the platform v_w, the grinding wheel speed w, the axial ultrasonic amplitude A, and the axial ultrasonic frequency f, the position of any point on the wheel surface with respect to the frame {G} origin is described by the following set of relations:

$$\begin{cases} x = x_0 + A\sin((2 \times pi \times f) \times t + \varphi_0) \\ y = y_0 \pm v_w \times t + (R + h_{ij}) \times \sin(\theta_{0j} - w \times t) \\ z = R - d - (R + h_{ij}) \times \cos(\theta_{0j} - w \times t) \end{cases} \quad (1)$$

Fig. 7 Schematic of axial UAG process

θ_{0j} initial angle of the jth row of the grinding wheel array
y_0 initial distance between the {O} and {G} origins in the Y direction
R nominal radius of the grinding wheel
h_{ij} height of the grinding wheel surface array at element (i, j)

In the process of small feed grinding, the protrusion height of the abrasive grain h_{ij} is small relative to the nominal radius of the grinding wheel R, and the included angle between the abrasive grain and the Z shaft is very small. This means that $(\theta_{0j} - w \times t)$ is small. In the grinding process, workpiece surface will produce a sinusoidal path when abrasives contact the workpiece surface. During this time, circular motion can be simplified to linear motion. Therefore, formula (1) is simplified to get formula (2):

$$\begin{cases} x = x_0 + A\sin((2pi \times f) \times t + \varphi_0) \\ y = y_0 \pm v_w \times t + (R + h_{ij}) \times (\theta_{0j} - w \times t) \\ z = R - d - (R + h_{ij}) \times \cos(\theta_{0j} - w \times t) \end{cases} \quad (2)$$

The wavelength of the sine shape grinding groove is different in down-grinding and up-grinding. It is generally known that the abrasive grain can easily enter into the cutting stage without the sliding stage or the plowing stage in down-grinding, which is similar to the numerical simulation method. Thus, down-grinding is used as the simulation processing method.

Based on the existing axial UAG device, the ultrasonic frequency is set to 20 kHz, the axial ultrasonic amplitude is 20 μm, and the grinding wheel is a cup wheel with a nominal radius of 60 mm. Due to the effects of feed depth and cutting angle on the grinding, the amplitude is $A + \frac{\sqrt{3}}{3} \times d$, and the wavelength of the sine shape grinding groove is $2 \times \left(R \times \left(w \times \frac{1}{2 \times f}\right) + v_w \times \frac{1}{2 \times f}\right)$. According to the geometric relations, the following formula can be obtained:

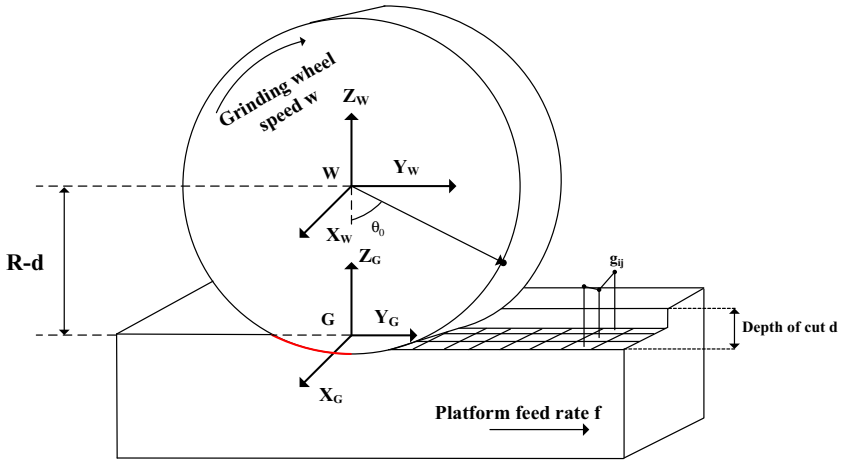

$$\tan(\theta/2) = \frac{\left(R \times \left(w \times \frac{1}{2 \times f}\right) + v_w \times \frac{1}{2 \times f}\right)}{\left(2 \times \left(A + \frac{\sqrt{3}}{3} \times d\right)\right)} \quad (3)$$

When the processing parameters are in accordance with formula (3), it can be guaranteed that the angle of crosshatch pattern is θ, and n is generated as 1478.6 r/min when v_w is temporarily taken as 8 m/min.

3.2 Governing equation of peak interval

In the single-pass grinding process, axial ultrasonic amplitude A is smaller than the grain distance within lines Δz. Therefore, only the grinding trajectories of the abrasive grain in the circumferential direction will overlap. When axial coordinates of the abrasive grains are close to each other, the peak interval ΔJ is close to the half sine grinding trajectory wavelength, and the crosshatch patterns are mutually interlaced. The wavelength of the sine shape grinding groove is 471 μm, using the motion equation in the previous section.

For the adjacent abrasive grain with the same axial coordinate, line distance Δx determines the interleaving degree of the grinding trajectory in the crosshatch micro structure. The formula of the circumferential distance between the two grinding trajectories Δy in the coordinate system of the workpiece surface is as follows:

$$\Delta y = v_w \times \frac{\Delta x \times 60}{R \times 2 \times \pi \times n} \quad (4)$$

The values of the grain distance within lines Δz, axial grain displacement between lines Δz_v, and circumferential distance Δy are set to 400, 80, and 235.5 μm (half of the sine grinding trajectory wavelength), respectively. That is, the axial coordinates of the abrasive grains which are separated by five columns are equal, so that Δxin formula (4) should be replaced by $5 \times \Delta x$. Taking Δx as 3000 μm and putting it into formulas 3 and 4, we can obtain that v_w is 8.735 m/min, and n is 1476.6 r/min. In these processing parameters, we can

Table 1 Major machining parameters

Grinding wheel	Grit size 100; grinding wheel radius 60 mm
Grinding wheel pattern parameters	Line distance Δ× 3000 μm; line angle a 50°; grain distance within lines 400 μm; axial grain displacement between lines Δz_v 80 μm
Grinding conditions	Grinding speed n 1476 r/min; cutting speed v_w 8.375 m/min; depth of cut 0.02 mm
Vibration conditions	Frequency f = 20 kHz; amplitude A = 20 μm
Grinding process	Surface grinding
Grinding method	Down-grinding
Transverse shifting distance	Average distribution of 0 to 100 μm

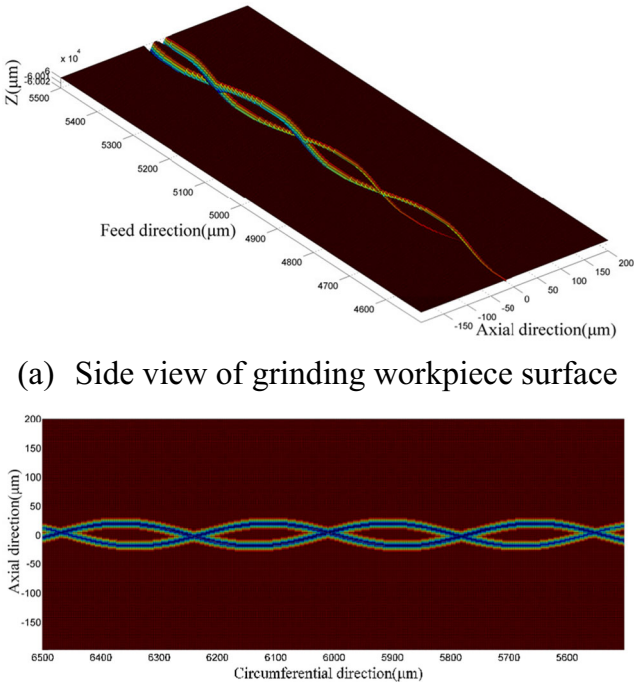

(a) Side view of grinding workpiece surface

(b) Top view of grinding workpiece surface

Fig. 8 Side and top views of simulated grinding workpiece surface

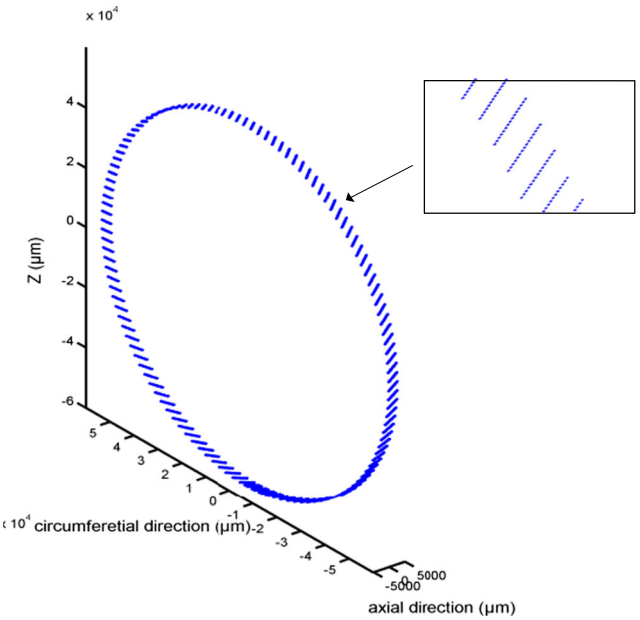

Fig. 9 Numerical model of ordered grinding wheel based on pattern parameters

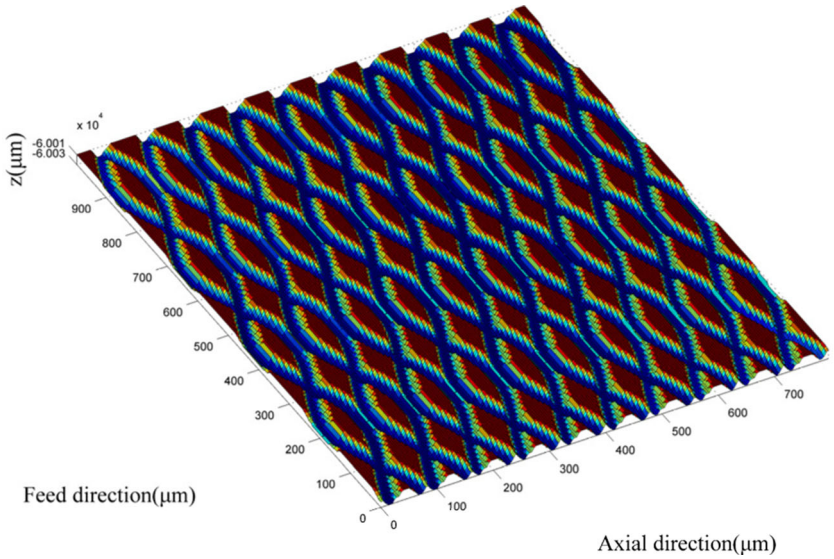

Fig. 10 Simulated single-pass grinding workpiece surface

not only ensure the angle of crosshatch pattern is 150° but also guarantee the crosshatch patterns are mutually interlaced.

3.3 Governing equation of angle between processing texture direction and sliding direction

As the active manufacturing crosshatch pattern is a symmetric structure, according to the experimental study [9], the service performance is good when the angle between the processing texture direction and the sliding direction is zero. The processing texture direction is directly related to the feed direction of grinding. We can guarantee the angle between the processing texture direction and sliding direction is zero when the feed direction of grinding is the same as the sliding direction (positive direction of Y axis in the frame {G}).

4 Numerical experiment verification about controllable generation of crosshatch surface

Because the fabrication technology of the ordered grinding wheel is not mature, the feasibility of the method is verified by numerical simulation. According to the angle of crosshatch pattern, the peak interval, and the angle between the processing texture direction and the sliding direction which are three active manufacturing characteristic parameters based on the service performance, the major machining parameters are obtained by inversely solving, as shown in Table 1.

Two abrasive grains, whose axial coordinates are equal but circumferential coordinates have a difference of 1500 μm, are used as the grinding wheel model. Then, the major machining parameters are put into the workpiece surface generation model, using the MATLAB programming, with reference to the CHEN

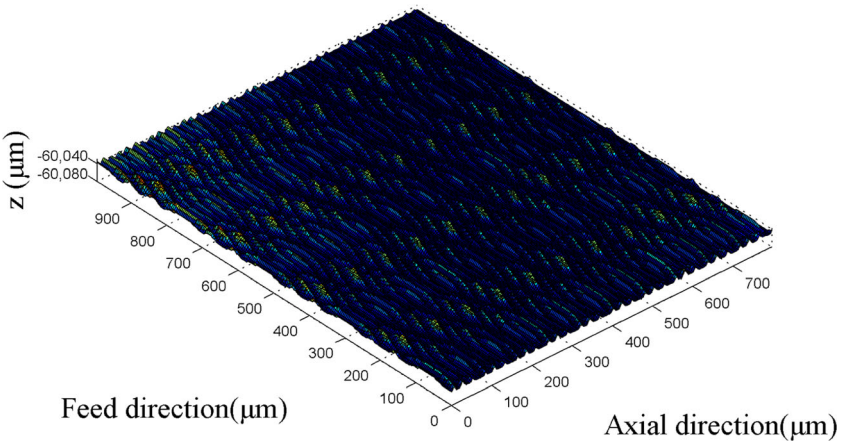

Fig. 11 Simulated multi-pass grinding workpiece surface

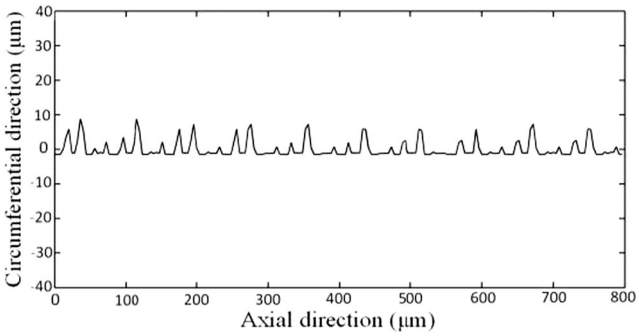

Fig. 12 Two-dimensional cross section of simulated grinding workpiece in axis direction

H [4]. The obtained workpiece surface has mutually interlaced grinding trajectories, as shown in Fig. 8. The sinusoidal grinding groove wavelength is 235.6 μm and the sinusoidal grinding groove amplitude is 31.8 μm using the matlab numerical calculation. So we can use formula 5 to calculate the angle θ.

$$\theta = 2 \times \arctan\left(\frac{l_{\text{wavelength}}}{2 \times l_{\text{amplitude}}}\right) \tag{5}$$

The calculated θ is 149.79°, and the error between the calculated value and the set value is 0.14%. It shows that the axis UAG can produce crosshatch pattern in these parameters, and it also indicates the set value of the line distance Δx is reasonable.

According to the pattern parameters of the grinding wheel, the numerical model of the grinding wheel is obtained, as shown in Fig. 9. The single-pass grinding surface has a uniform and staggered crosshatch micro structure, as shown in Fig. 10. The distance between adjacent UAG trajectories is very small, meeting the design requirement. Meanwhile, the feed direction of grinding is the same as the sliding direction, which meets the setting of the angle between the processing texture direction and the sliding direction.

The multi-pass grinding surface can also be obtained in the above major machining parameters, as shown in Fig. 11.

Fig. 13 Working surface of conventional grinding wheel

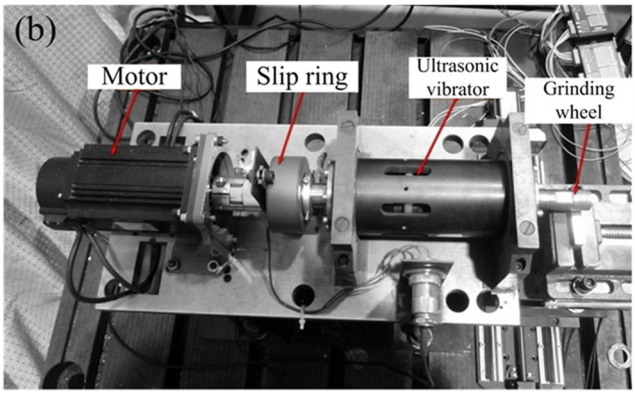

Fig. 14 Experimental setup of ultrasonic-assisted grinding

Multi-pass grinding makes the region polished where single-pass grinding has no effect on so that the surface roughness is decreased. Compared with conventional grinding, the active manufacturing UAG workpiece surface has crosshatch micro structure which is different from the parallel grooves.

As shown in Fig. 12, the two-dimensional cross section of the grinding workpiece in the axis direction of the grinding wheel, with the roughness Ra as 1.12 μm in the sampling length of 800 μm, is different from that in the conventional grinding. Due to the axial movement of the abrasive grains, the workpiece in the axis direction of the grinding wheel is removed in some degree. There are some relatively flat areas in the two-dimensional cross section of the grinding workpiece, which is the main reason why the surface roughness of the workpiece is reduced effectively by the axial UAG.

In the above, single-pass grinding and multi-pass grinding are simulated through three characterization parameters to verify the feasibility of the active manufacturing based on the workpiece surface service performance. However, because the sliding, plowing, and cutting stages as well as the fracture and wear phenomenon of the grains are not considered, the two-dimensional section and three-dimensional surface of the workpiece appear great regularity. The next step is to create an optimization model of the workpiece surface by adding the

Table 2 Major machining parameters

Processing conditions	Parameters of Fig. 15
Grinding wheel radius	12 mm
Grain size	200
Amplitude	10 μm
Frequency	20 kHz
Depth of cut	5 μm
Cutting speed	4 mm/s
Grinding wheel speed	1500 rpm
Processing equipment	YP4020-4P ultrasonic grinding machine
Workpiece material	C45 carbon steel

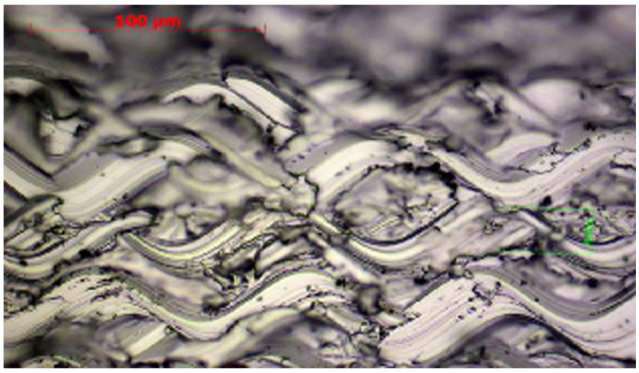

Fig. 15 Axial UAG surface with mutually interlaced grinding trajectories

factors which are not considered in the grinding process, so that the formation mechanism of the workpiece surface is more consistent with the actual situation.

Because the fabrication technology of the ordered grinding wheel is not mature, grinding experiment of electroplated diamond grinding wheel was used to verify the feasibility of the new method.

Figures 13 and 14 show the photographs of the working surface of conventional grinding wheel and experimental setup.

Table 2 shows the main processing parameters of grinding.

Figure 15 is workpiece surface, and it can be found that under certain conditions, abrasive grinding trajectories are staggered to form a crosshatch microstructure.

First of all, given crosshatch microstructure can be generated with requested parameters by using the numerical simulation method. And at the same time, it was found that when the distance between two abrasive grains is a certain value, a crosshatch microstructure can be found on the ultrasonic grinding workpiece surface. So it verifies the feasibility of the method.

5 Conclusions

(1) According to the kinematics of grinding, the mapping relationship between process parameters and characteristic parameters is established to achieve the active manufacturing of the crosshatch micro structure.

(2) Because the fabrication technology of the ordered grinding wheel is not mature, the feasibility of the method is verified by numerical simulation. A comparison is made between the set value and simulated value of the characteristic parameters. At the same time, grinding experiment of electroplated diamond grinding wheel can illustrate the feasibility of the new method.

(3) The next step is to make further verification of the feasibility of the new method by fabricating ordered grinding wheel, and build quantitative relationship between the surface characteristic parameters and causative performance to achieve active manufacturing driven by performance.

Funding information The study was financially supported by the National Natural Science Foundation of China (NSFC) through Grant Nos. 51535012, 51605160, and U1604255; the Key Research and Development Project of Hunan Province through Grant No. 2016JC2001; the Open Research Fund of Key Laboratory of High Performance Complex Manufacturing, Central South University (No. Kfkt2016-8); and Independent Exploration Innovative Projects of Central South University (2017zzts414).

References

1. Evans CJ, Bryan JB (1999) "Structured", "textured" or "engineered" surfaces. CIRP Ann Manuf Technol 48(2):541–556. https://doi.org/10.1016/s0007-8506(07)63233-8
2. Alting L, Kimura F, Hansen HN, Bissacco G (2003) Micro engineering. CIRP Ann Manuf Technol 52(2):635–657. https://doi.org/10.1016/s0007-8506(07)60208-x
3. De Chiffre L, Kunzmann H, Peggs GN, Lucca DA (2003) Surfaces in precision engineering, microengineering and nanotechnology. CIRP Ann Manuf Technol 52(2):561–577. https://doi.org/10.1016/s0007-8506(07)60204-2
4. Chen H, Tang J (2014) A model for prediction of surface roughness in ultrasonic-assisted grinding. Int J Adv Manuf Technol 77(1–4):643–651. https://doi.org/10.1007/s00170-014-6482-3
5. Chen H, Tang J, Zhou W (2013) An experimental study of the effects of ultrasonic vibration on grinding surface roughness of C45 carbon steel. Int J Adv Manuf Technol 68(9–12):2095–2098. https://doi.org/10.1007/s00170-013-4824-1
6. Zhou W, Tang J-Y, He Y-F, Liao D-R (2015) Associated rules between microstructure characterization parameters and contact characteristic parameters of two cylinders. J Cent South Univ 22(11):4228–4234. https://doi.org/10.1007/s11771-015-2971-2
7. Suh MS, Chae YH (2008) Friction characteristic of sliding direction and angle of micro-grooved crosshatch patterns under lubricated contact. Adv Mater Res 47-50:507–510. https://doi.org/10.4028/www.scientific.net/AMR.47-50.507
8. M-s S, Y-h C, S-s K, Hinoki T, Kohyama A (2010) Effect of geometrical parameters in micro-grooved crosshatch pattern under lubricated sliding friction. Tribol Int 43(8):1508–1517. https://doi.org/10.1016/j.triboint.2010.02.012
9. Yuan S, Huang W, Wang X (2011) Orientation effects of micro-grooves on sliding surfaces. Tribol Int 44(9):1047–1054. https://doi.org/10.1016/j.triboint.2011.04.007
10. Yousfi M, Mezghani S, Demirci I, El Mansori M (2016) Tribological performances of elliptic and circular texture patterns produced by innovative honing process. Tribol Int 100:255–262. https://doi.org/10.1016/j.triboint.2016.01.049
11. Klink U, Sandhof G (1991) Method and tool for machining the surfaces of workpieces. Google Patents,
12. Liu K, Lauwers B, Reynaerts D (2009) Process capabilities of micro-EDM and its applications. Int J Adv Manuf Technol 47(1–4):11–19. https://doi.org/10.1007/s00170-009-2056-1
13. Wang Y, Lin B, Cao X, Wang S (2014) An experimental investigation of system matching in ultrasonic vibration assisted grinding for titanium. J Mater Process Technol 214(9):1871–1878. https://doi.org/10.1016/j.jmatprotec.2014.04.001

14. Tawakoli T, Azarhoushang B (2009) Effects of ultrasonic assisted grinding on CBN grinding wheels performance. 209–214. doi: https://doi.org/10.1115/msec2009-84186
15. Warnecke G, Zitt U (1998) Kinematic simulation for analyzing and predicting high-performance grinding processes. CIRP Ann Manuf Technol 47(1):265–270. https://doi.org/10.1016/s0007-8506(07)62831-5
16. Cooper WL, Lavine AS (2000) Grinding process size effect and kinematics numerical analysis. J Manuf Sci Eng 122(1):59. https://doi.org/10.1115/1.538888
17. Zhou X, Xi F (2002) Modeling and predicting surface roughness of the grinding process. Int J Mach Tools Manuf 42(8):969–977. https://doi.org/10.1016/s0890-6955(02)00011-1
18. Hecker RL, Ramoneda IM, Liang SY (2003) Analysis of wheel topography and grit force for grinding process modeling. J Manuf Process 5(1):13–23. https://doi.org/10.1016/s1526-6125(03)70036-x
19. Malkin S (1989) Grinding technology: theory and applications of machining with abrasives. Halsted Press, E. Horwood
20. Sung CM (1999) Brazed diamond grid: a revolutionary design for diamond saws. Diam Relat Mater 8(8–9):1540–1543. https://doi.org/10.1016/s0925-9635(99)00086-2
21. Aurich JC, Herzenstiel P, Sudermann H, Magg T (2008) High-performance dry grinding using a grinding wheel with a defined grain pattern. CIRP Ann Manuf Technol 57(1):357–362. https://doi.org/10.1016/j.cirp.2008.03.093
22. Aurich JC, Braun O, Warnecke G, Cronjäger L (2003) Development of a superabrasive grinding wheel with defined grain structure using kinematic simulation. CIRP Ann Manuf Technol 52(1):275–280. https://doi.org/10.1016/s0007-8506(07)60583-6
23. Koshy P, Iwasald A, Elbestawl MA (2003) Surface generation with engineered diamond grinding wheels: insights from simulation. CIRP Ann Manuf Technol 52(1):271–274. https://doi.org/10.1016/s0007-8506(07)60582-4